

Demonstrating Quantum Scaling Advantage in Approximate Optimization for Energy Coalition Formation with 100+ Agents

Naeimeh Mohseni,¹ Thomas Morstyn,² Corey O’Meara,¹ David Bucher,³ Jonas Nüßlein,⁴ and Giorgio Cortiana¹

¹*E.ON Digital Technology GmbH, Hannover, Germany*

²*Department of Engineering Science, University of Oxford, UK*

³*Aqarios GmbH, Prinzregentenstraße 120, Munich, Germany*

⁴*Ludwig-Maximilians University Munich, Institute for Computer Science, Germany*

The formation of energy communities is pivotal for advancing decentralized and sustainable energy management. Within this context, Coalition Structure Generation (CSG) emerges as a promising framework. The complexity of CSG grows rapidly with the number of agents, making classical solvers impractical for even moderate sizes. This suggests CSG as an ideal candidate for benchmarking quantum algorithms against classical ones. Facing ongoing challenges in attaining computational quantum advantage for exact optimization, we pivot our focus to benchmarking quantum and classical solvers for approximate optimization. Approximate optimization is particularly critical for industrial use cases requiring real-time optimization, where finding high-quality solutions quickly is often more valuable than achieving exact solutions more slowly. Our findings indicate that quantum annealing (QA) on DWave can achieve solutions of comparable quality to our best classical solver, but with more favorable runtime scaling, showcasing an advantage. This advantage is observed when compared to solvers, such as Tabu search, simulated annealing, and the state-of-the-art solver Gurobi in finding approximate solutions for energy community formation involving over 100 agents. DWave also surpasses 1-round QAOA on IBM hardware. Our findings represent the largest benchmark of quantum approximate optimizations for a real-world dense model beyond the hardware’s native topology, where D-Wave demonstrates a scaling advantage.

I. INTRODUCTION

To explore the potential of quantum computing in optimization problems it is encouraging to benchmark quantum solvers against classical solvers in tackling problems that are sufficiently hard and exceed the capabilities of state-of-the-art classical solvers. This exploration becomes even more intriguing when problems get already hard in intermediate sizes where existing quantum hardware can be effectively leveraged. It is also crucial that the problem can be formulated compatible with existing quantum algorithms and hardware [1]. As we explain next, energy coalition formation applying the Coalition Structure Generation (CSG) game stands out as an exemplary candidate for such benchmarking, given its computational complexity and profound real-world significance within the industry. The formation of energy communities represents a significant step towards decentralized and sustainable energy management, offering opportunities for local empowerment, renewable energy adoption, and enhanced resilience in energy systems [2–6].

CSG provides a framework for understanding how agents, can form coalitions denoted by C_l (with l being the index of the coalition) to optimize their collective benefits [7–10]. A coalition within this context can be characterized by a characteristic function, typically denoted as $v(C_l)$, which assigns values to different coalitions. The value function provides a measure of the cooperative advantage or payoff that the agents in the coalition can attain by working together, as opposed to operating independently [11, 12].

The task of creating coalition structures is highly challenging, especially given the presence of n agents, lead-

ing to a staggering $O(n^n)$ possible partitions. Currently, the only algorithm capable of finding an optimal solution is the Dynamic Programming algorithm, achieving this in $O(3^n)$ time [13]. This approach is limited to systems consisting of a few tens of agents (i.e. $n < 25$). CSG can be transformed into an approximately equivalent game represented using the induced subgraph game (ISG) [14]. In this representation, nodes correspond to agents, and coalition values are reflected in pairwise interactions within a weighted graph, such that $v(C_l) = \sum_{(i,j) \in C_l} w_{ij}$ [11, 12]. The transformation of CSG to ISG allows the problem to be recast as quadratic unconstrained binary optimization (QUBO), enabling more computationally efficient approaches. Nonetheless, it is crucial to note that the problem remains NP-complete [11] such that leading classical solvers, such as DyCE [15] and CFSS [15] are limited in scalability and memory requirements. For instance, DyCE [15], which employs dynamic programming, is restricted to systems with around 25 agents due to its exponential memory complexity ($O(2^n)$) and lacks an anytime approach. CFSS can handle larger but shallow problems, yet still explores all possible solutions for complete graphs with a complexity of $O(n^n)$.

In this work, we propose a novel formulation of energy coalition formation that can be encapsulated within the framework of CSG. We first introduce a novel method for transforming the CSG formulation into an ISG. Building on this transformation, we apply the approximation introduced in [16], under which our problem reduces to an iterative weighted minimum cut on the ISG (formulated as a QUBO). The complexity of finding an optimal solution for this reduced formulation remains $O(n^3)$. We show a solution where its optimality is not proven can be

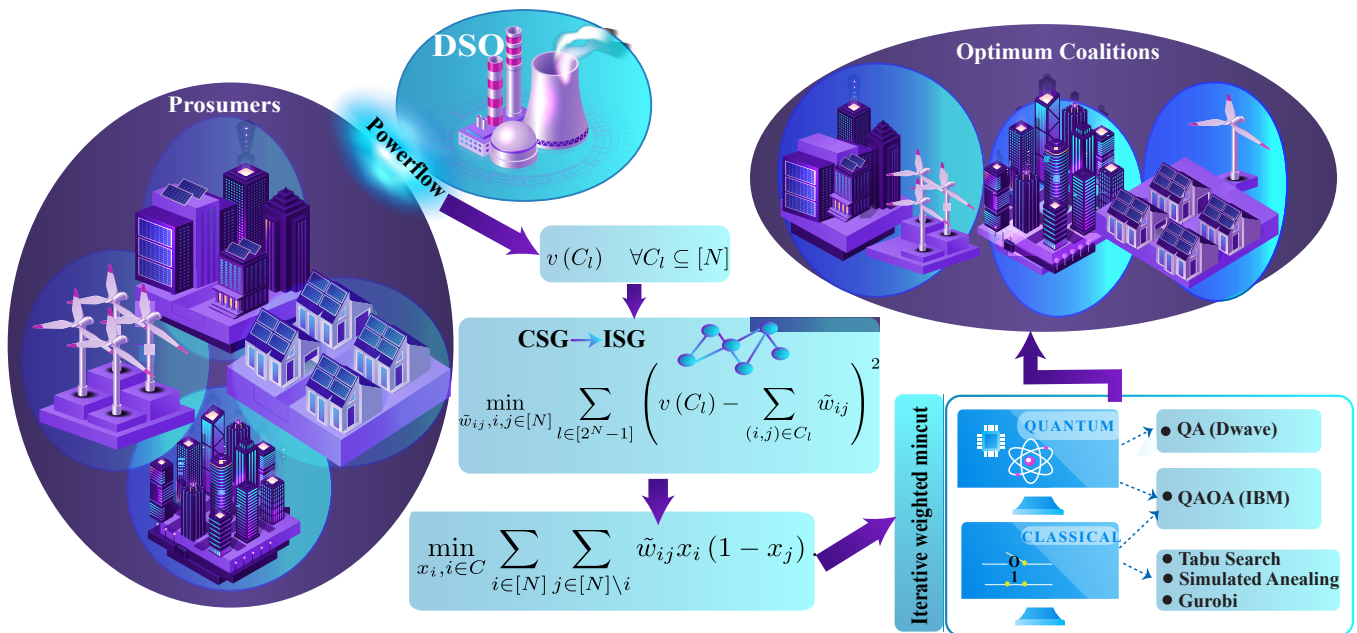


Figure 1. (a) Schematic representation of the workflow: The Distribution System Operator (DSO) strategically evaluates the potential of prosumer communities, aiming to minimize network management costs through optimized power flow analysis. The DSO’s decision-making involves partitioning prosumers into net-metered coalitions, treating it as a Coalition Structure Generation (CSG) problem to optimize overall network efficiency. We transform the CSG formulation into the Induced Subgraph Game (ISG). An approximate solution to the ISG is found through iterative splitting coalitions to bipartitions until no value-increasing bipartitions remain. In the benchmarking phase, the efficiency of both quantum and classical solvers is assessed in the iterative splitting process.

found in polynomial time.

Our performance evaluation involves benchmarking quantum annealing on DWave hardware and the Quantum Approximation Optimization Algorithm (QAOA) on IBMQ hardware against classical solvers such as Gurobi [17], Tabu search [18], simulated annealing [19], and QBSolve [20]) to find approximate solutions. We provide preliminary empirical evidence suggesting a potential scaling advantage of DWave for a dense, real-world problem in *approximate optimization*. A recent study [21] applying quantum annealing correction demonstrates a scaling advantage for approximate optimization against parallel tempering with isoenergetic cluster moves. However, that work is limited by the problem’s compatibility with the hardware’s connectivity and is focused on a 2D model, which restricts its range of applications. We also show Dwave outperforms 1-round QAOA on IBM Hardware.

Additionally, our experiments demonstrate that the solutions obtained through approximation on the ISG remain remarkably close to those derived from the original CSG formulation (up to system sizes that we have been able to check). This showcases the robustness and efficacy of our new introduced method in transferring CSG to ISG.

II. PROBLEM FORMULATION

Consider a distribution network with N prosumers (proactive consumers), each with some combination of inflexible loads, flexible loads, generation and/or storage. A standard arrangement for retail contracts is for each prosumer’s energy demand to be individually metered, with the net demand during each metering period t charged at an import price λ_t^b , and net supply rewarded at a lower export price $\lambda_t^s \leq \lambda_t^b$. An alternate arrangement is to enable groups of retail prosumers to form net-metered energy communities, where prosumers’ collective net demand is metered. This creates an overall incentive for community supply-demand balancing, and cooperative game theory can be used to calculate cost/revenue sharing which aligns individual incentives with collective optimization. The energy management problem for each coalition with optimization horizon $[T]$, can be generically described by,

$$\begin{aligned}
& \min_{p_i, i \in [C_l]} \left(\sum_{i \in [C_l]} c_i(p_i) \right. \\
& \quad \left. - \Delta_t \sum_{t \in [T]} \left(\lambda_t^b \left[\sum_{i \in [C_l]} p_{it} \right]^- + \lambda_t^s \left[\sum_{i \in [C_l]} p_{it} \right]^+ \right) \right) \\
& \text{s.t. } p_i \in \mathcal{P}_i, \forall i \in [C_l].
\end{aligned} \tag{1}$$

$c_i(p_i)$ presents each prosumer's cost function associated with the usage of their flexible devices and a constraint set \mathcal{P}_i for their output power vector, which may be time-coupled. For the exact choice of $c_i(p_i)$ and constraint set \mathcal{P}_i , refer to Supplemental Material Sec. II. We label the N coalitions for which prosumers are metered individually C_i^0 . We remind that C_i refers to i -th coalition. $p_i = (p_{i1}, \dots, p_{iT})$ is the vector of output powers over the time horizon and p_{it} is the prosumer output power during time interval t . $[p_{it}]^+ = \max\{0, p_{it}\}$ and $[p_{it}]^- = \min\{0, p_{it}\}$. Δ_t is the duration of each time interval.

The supply-demand balancing incentivized by community net metering is generally desirable for local groups of prosumers. However, when expanded to larger more dispersed groups, there is the potential that this will introduce distribution losses and the need for additional flexibility procurement to prevent network constraint violations. Consider the perspective of a distribution system operator (DSO), and assume it has the authority to allow or disallow the formation of net-metered energy communities. The DSO needs to be able to calculate the value in terms of reduced network management costs (which could be negative) of allowing a coalition of prosumers C_l to form a net-metered community. In general, network power flows and management costs will depend on the collective operation of all prosumers. To simplify the value calculation for coalition formation, we focus on the marginal value created assuming prosumers which are not in the coalition operate under individual metering. In this case, the value created can be approximated as,

$$\begin{aligned}
v(C_l) &= \mathcal{O}^{opf*}(p_i^{\text{ind}*} \mid i \in [N]) - \mathcal{O}^{opf*}(p_i^{\text{net}*} \mid i \in [N]), \\
p_i^{\text{ind}*} &= p_i^* \text{ from (1) optimized for } C_i^0, \\
p_i^{\text{net}*} &= \begin{cases} p_i^* \text{ from (1) optimized for } C_l, & \text{if } i \in C_l, \\ p_i^* \text{ from (1) optimized for } C_i^0, & \text{otherwise} \end{cases}
\end{aligned} \tag{2}$$

Here, $*$ indicates the solution to an optimization problem. $p_i^{\text{ind}*}$ ($p_i^{\text{net}*}$) represents the optimized power for the prosumer i under individual (net) metering. $[N] = \{1, 2, \dots, N\}$ and \mathcal{O}^{opf*} is the objective function value for the following optimal power flow problem which the DSO can use to procure flexibility to manage losses and network constraints,

$$\begin{aligned}
& \min_{p_{kt}^\uparrow, p_{kt}^\downarrow, k \in [K], t \in [T]} \Delta_t \sum_{t \in [T]} \sum_{k \in [K]} \lambda_{kt}^\uparrow p_{kt}^\uparrow + \lambda_{kt}^\downarrow p_{kt}^\downarrow \\
& \text{s.t. } \left\{ p_{kt}^\uparrow, p_{kt}^\downarrow \mid k \in [K] \right\} \in \mathcal{N}_t(p_{it}^* \mid i \in [N]), \forall t \in [T], \\
& \quad \left\{ p_{kt}^\uparrow, p_{kt}^\downarrow \mid t \in [T] \right\} \in \mathcal{P}_k^{\uparrow\downarrow}, \forall k \in [K].
\end{aligned} \tag{3}$$

$p_{kt}^\uparrow, p_{kt}^\downarrow$ are the costs of upward/downward flexibility at network node $k \in [K]$ during time interval $t \in [T]$, and $\lambda_{kt}^\uparrow, \lambda_{kt}^\downarrow$ are the associated prices. \mathcal{N}_t is the network constraint set for time interval t (e.g. nodal power balance, bus voltage limits, line power flow limits). Note that this constraint set will depend on the prosumer output powers from the retail market $p_{it}^*, i \in [N]$. $\mathcal{P}_k^{\uparrow\downarrow}$ is the constraint set for flexibility at network node k , which in general may be time-coupled. For more details on power flow optimization refer to Sec. II of supplemental Material.

The DSO decision problem is then to partition the prosumers into a set of net-metered coalitions with the goal of minimizing network management costs. This is formulated as a CSG problem, which can be solved using binary integer linear programming (BILP) [22],

$$\begin{aligned}
& \max_{x_l, l \in [2^N - 1]} \sum_{l \in [2^N - 1]} v(C_l) x_l, \\
& \text{s.t. } \sum_{i \in [2^N - 1]} S_{il} x_l = 1, \forall i \in [N], \\
& \quad x_l \in \{0, 1\}, \forall l \in [2^N - 1].
\end{aligned} \tag{4}$$

Note that there are $2^N - 1$ potential sub-coalitions of prosumers. $S_{il} = 1$ if prosumer $i \in [N]$ belongs to coalition C_l (i.e. $i \in C_l$), and $S_{il} = 0$ otherwise. Binary decision variable $x_l = 1$ indicates that C_l is part of the selected partition, and the value function $v(C_l)$ gives the value of the coalition. This formulation is computationally intensive since the number of binary decision variables depends on the number of sub-coalitions, which increases exponentially with the number of prosumers (i.e. $2^N - 1$).

This CSG formulation can be transformed into ISGs, where the value of a coalition can be expressed as the sum of pair-wise ‘‘joint utilities’’ between prosumers $w_{ij} \in \mathbb{R}, i, j \in [N]$, i.e. $v^{\text{ISG}}(C_l) = \sum_{(i,j) \in C_l} w_{ij}$ with lower computational requirements. The value function nonlinearities mean this framework is not directly applicable to our CSG. However, we can make use of an ISG based on pairwise joint utilities \tilde{w}_{ij} which approximate our CSG. The following quadratic programming problem can be used to find pairwise weights that minimize the mean squared error between the value functions and an approximate ISG,

$$\min_{\tilde{w}_{ij}, i, j \in [N]} \sum_{l \in [2^N - 1]} \left(v(C_l) - \sum_{(i,j) \in C_l} \tilde{w}_{ij} \right)^2. \tag{5}$$

Starting with the grand coalition, an approximate solution to the ISG can be found by iteratively splitting

coalitions in two, until no value-increasing bipartitions are available [16]. For a given iteration, let C , be one of the optimal bipartitions that was found for our N prosumers. The optimal bipartitions of C at the next iteration can be found using the following quadratic unconstrained binary optimization (QUBO) with N binary decision variables x_i ,

$$\begin{aligned} \min_{x_i, i \in C} & \sum_{i \in [N]} \sum_{j \in [N] \setminus i} \tilde{w}_{ij} x_i (1 - x_j). \\ \text{s.t. } & x_i \in \{0, 1\}, \forall i \in [N]. \end{aligned} \quad (6)$$

Here the binary vector $\mathbf{x} = [x_1, x_2, \dots, x_N]$ for N prosumers encodes the bipartition: prosumers with the same value of x_i belong to the same subcoalition. For example, $\mathbf{x} = [1, 0, 0, 1]$ indicates that prosumers 1 and 4 form one subcoalition, while prosumers 2 and 3 form the other.

The schematic representation of the full workflow is shown in Fig. 1.

III. RESULTS

In this section, we elaborate on the outcome of our performance evaluation, benchmarking an exact classical solver, the commercial state-of-the-art classical solver Gurobi, and QB-solve [20] against quantum annealing on DWave hardware (DWave Advantage 4.1), and 1-round QAOA on IBMQ hardware (IBM-Osaka). For a detailed overview of all the solvers utilized in our benchmarking, refer to Supplemental Material Sec. I. Before presenting the benchmarking results, it is essential to elucidate the structure and complexity of the problem instances generated from our use case as follows.

Problem complexity: Our analysis reveals that the graphs resulting from the mapping of CSG to ISG are very dense across all system sizes, with connectivity levels exceeding 90 percent. Moreover, the weight distribution includes both positive and negative values forming a Gaussian distribution centered closely around zero. The light blue histogram depicted in Fig. 2 lower right panel illustrates the weight distribution for the case of 18 prosumers averaging over 20 instances (different instances of the problem correspond to different initial power configurations for prosumers at the outset and varying export and import prices). This scenario, characterized by a dense graph featuring a mixture of positive and negative weights, represents a particularly challenging case [23]. For further insights, refer to [23], where they discuss the boundary between polynomially-solvable Max Cut and NP-Hard Max Cut instances when they are classified only on the basis of the sign pattern of the objective function coefficients.

Solver compatibility: When benchmarking algorithms, selecting the appropriate formulation for each solver is crucial to ensure their optimal performance. Our problem formulation here namely the QUBO formulation

is well-suited to all the solvers we are applying in this work.

Benchmark metrics: We benchmark the performances in terms of solution quality and running time (Fig. 2). The runtime for all solvers includes also any classical processing time, such as the time spent optimizing variational parameters. The results for each number of prosumers showcase averages across 20 realizations except for IBM hardware and random solver with 2^{12} shots where results are shown for a single problem instance per data point.

Solution quality: In Fig. 2(a), we present the solution quality defined as the ratio of the optimal coalition values obtained by any solver on ISG formulation to the values found by Gurobi on the same formulation. Up to this size, Gurobi is still able to prove the optimality of the solutions found. For the prosumer sizes studied here (up to 45), both DWave and our classical solver consistently match Gurobi's solution. In contrast, the 1-round QAOA exhibits a significant decline in solution quality as system size increases and its performance is indistinguishable from a random solver. In some cases, QAOA performs slightly better than a random sampler but mostly its performance is indistinguishable from a random solver.

Here QAOA is enhanced with Fire Opal's error suppression pipeline, excluding any readout mitigation and postprocessing. This incorporates automated error-suppression techniques, such as layout optimization [24], dynamical decoupling for crosstalk and dephasing suppression [25], and AI-driven gate waveform optimization.

Several factors contribute to the suboptimal performance of QAOA on IBM hardware. The most significant one is that the traditional QAOA ansatz is inefficient and not hardware-friendly for dense problems like ours. In Fig. 2 (d), we compare the circuit depth applying the Fire Opal transpiler and the default Qiskit transpiler, showing that circuit depth increases quadratically with the number of qubits using Qiskit's default. While Fire Opal's transpilation significantly reduces the circuit depth and improves scaling, it still remains insufficient to make QAOA competitive for dense problems, given current gate fidelities [26, 27]. Recent studies have proposed hardware-friendly modifications to the QAOA ansatz [28, 29], but their effectiveness for dense models remains elusive.

We also investigate the closeness of the solution derived from the ISG transformation to that derived from the original CSG formulation in Panel (b). In this case, the solution quality is defined as the ratio of the optimal coalition value obtained from any solver on ISG to the exact solution of the original CSG formulation determined by improved dynamic programming (IDP) [13]. IDP is the only existing algorithm capable of finding an optimal solution for the CSG formulation. However, the runtime scales as $O(n^3)$, allowing us to calculate the solution quality for up to 20 prosumers. It is very encouraging to see that solutions obtained through approximation on the ISG remain remarkably close to those derived from the original CSG formulation. This confirms the efficacy of

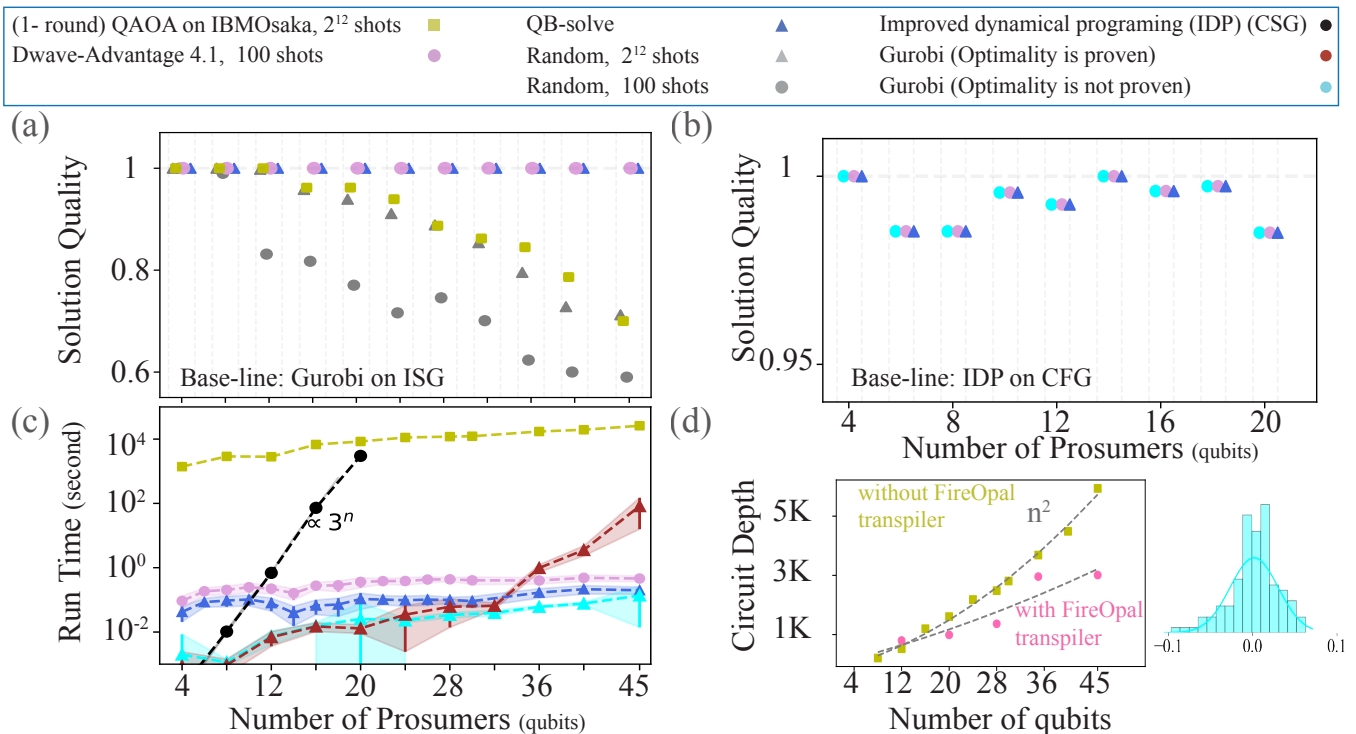


Figure 2. Benchmarking classical solvers against quantum solvers in energy coalition formation: (a) Solution quality of different solvers on ISG formulation where the baseline is w.r.t. the solution determined with the Gurobi on the same formulation. (b) The solution quality of different solvers on ISG formulation w.r.t. the solution determined with IDP on the original CSG formulation. (c) Run time of different solvers on ISG formulations as well as run time of improved dynamical programming (IDP) on CSG formulation. (d) QAOA circuit depth on quantum hardware for different numbers of prosumers (number of qubits). Note that results for each number of prosumers showcase averages across 20 realizations except for IBM hardware and random solver with 2^{12} shots where results are shown for a single problem instance per data point. The light blue histogram on the lower right shows the weight distribution after transferring CSG to ISG.

the mapping that we introduced in Eq. 5.

Run Time: Fig. 2 (c), shows the run time of different solvers. DWave and QB-Solve demonstrate competitive runtimes, but clear scaling is difficult to observe with up to 45 prosumers. For Gurobi, we report two runtimes: the cyan line represents the time taken to find a solution that no longer improves over time, though its optimality is not proven. The brown line shows the total runtime, including the time spent proving the solution’s optimality. As the number of prosumers increases, it becomes increasingly challenging for Gurobi to confirm optimality. For instances with more than 50 prosumers, Gurobi is unable to prove optimality even after several hours of computation. IDP on CSG also experiences a noticeable increase in runtime as the problem size grows.

Interestingly, the scaling behavior of QAOA on Hardware is close to DWave and QB-solve, albeit with a significantly larger prefactor. This can be attributed to iteratively updating variational parameters and running the algorithm on hardware for each parameter update. Initializing variational parameters based on existing heuristic schemes [30, 31] or learning them via machine learning

techniques [32–34] could potentially reduce this prefactor to some extent.

To compare our solvers effectively, it is essential to consider both runtime and solution quality together. For problem sizes up to 45 prosumers, both D-Wave and our classical solver consistently achieve matching solutions; however, runtime comparisons at this scale do not provide reliable insights into scaling behavior. Our problem instances become difficult to solve beyond 50 prosumers, where even Gurobi struggles to find optimal solutions. Therefore, drawing firm conclusions about performance requires exploring larger instances, which we address next.

Randomly generated problems: To enhance the robustness of our findings and gain deeper insights into the performance scalability of DWave, we validate our results on larger-scale random problems by generating our problem instances randomly. Solving power flow equations for more than a few tens of prosumers (required to generate problem instances) demands substantial computational resources, and for the scope of this work, random generation suffices. For smaller numbers of prosumers, the distribution of generated problems, after transforming

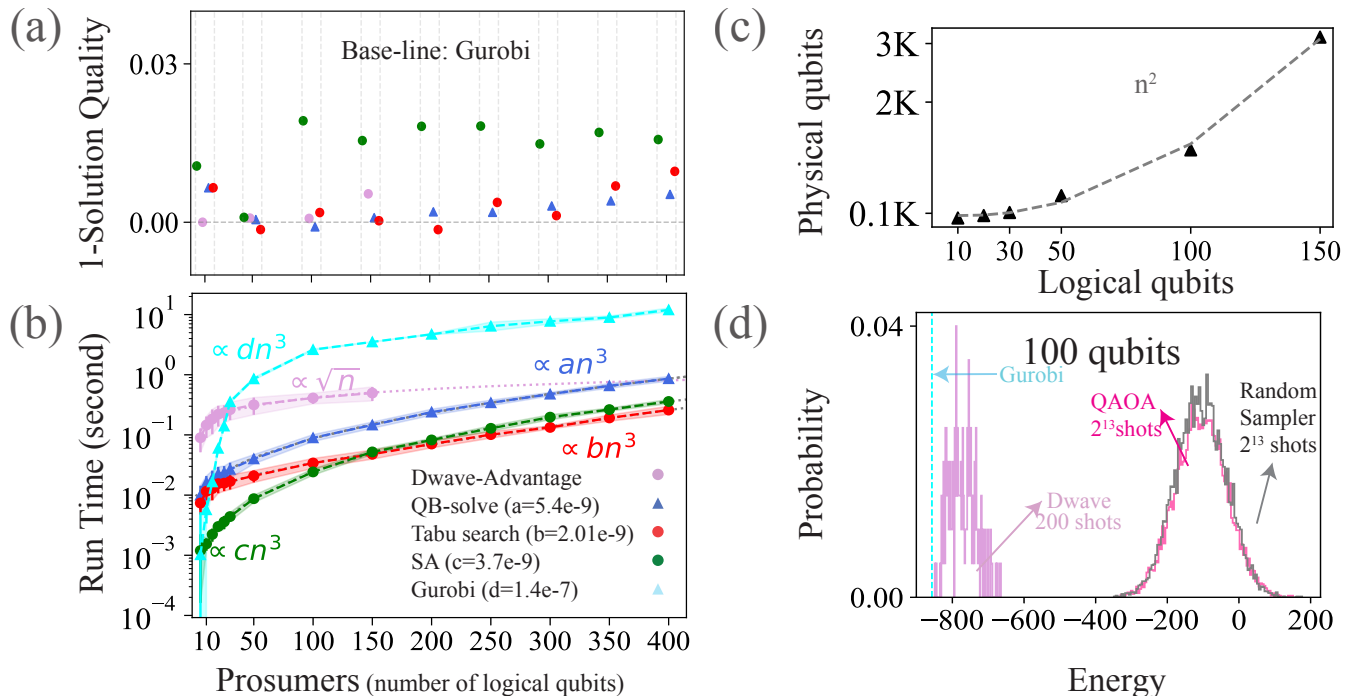


Figure 3. Benchmarking classical solvers against DWave in energy coalition formation for randomly generated problem instances. (a) The solution quality versus the number of prosumers. (b) Run time versus number of prosumers. (c) The number of physical qubits versus logical qubits (number of prosumers) on DWave hardware for the first split of the grand coalition into two partitions. Note that results for each number of prosumers showcase averages across 20 realizations. (d) Energy distribution sampled from DWave, QAOA, and a random sampler for the first split of the grand coalition to two partitions for a randomly generated instance with 100 prosumers (100 qubits). The dashed vertical line shows the solution found by Gurobi.

from CSG to ISG, follows a Gaussian distribution centered around zero with a width of 0.2 across all prosumer sizes. Therefore, for larger sizes (above 22 prosumers), we generate our problem instances using the same Gaussian distribution but intentionally vary the width to 2. This deliberate variation allows us to investigate the correlation between solvers' performance and distribution characteristics, which may align with different choices of constraints and parameters in the problem formulation.

The outcome of this investigation is presented in Fig. 3. For a more comprehensive benchmark, we additionally employ two other classical solvers: simulated annealing and Tabu search. For instances with more than 50 prosumers, Gurobi fails to find a provably optimal solution and fails to terminate even after several hours of computation. Additionally, we observed that the objective value no longer improves significantly after some time. Therefore, we introduced a termination criterion: the optimization process is stopped when the change in the objective value is less than $1e-8$, and no significant improvement is observed within a predefined time window of 1 second. Note that if no improvement occurs within this 1-second window, the time is not included in the reported runtime. We consider the best solution found by Gurobi as the reference, even though its optimality

remains unproven and other solvers may find a better solution.

The optimality gap—the difference between the best solution found by the solver and the upper bound of the optimal solution, derived from the dual problem—varies across different problem instances and iterations, particularly during the process of splitting coalitions into bipartite groups. We report the optimality gap for the first iteration, namely the initial split of the grand coalition into two partitions. Averaged across all problem instances, the gap is 17%, 26%, 25%, 29%, 28%, 30%, 29% for prosumer sizes of 50, 100, 150, 200, 250, 300 and 350, respectively. In most cases, the optimality gap reaches zero in later iterations.

DWave consistently demonstrates performance in line with the results depicted in Fig. 2 and competes effectively with the classical solvers. In terms of solution quality, for problem sizes up to 150 prosumers, the largest scale tested on the hardware, DWave consistently finds solutions similar to those obtained by Gurobi, except for the case with 150 prosumers, where DWave's solution is 1% suboptimal. Within this range of prosumers, Tabu search consistently finds solutions that are either slightly better or worse than those found by Gurobi, within less than 1% difference. For instances with over 200 prosumers, where

no results are available from D-Wave, Gurobi consistently identifies the best solution among classical solvers, and all solvers outperform SA.

In terms of run time, DWave demonstrates a more favorable runtime scaling as a function of problem size, as depicted in Fig. 3(b). The runtime of Gurobi, QB-solve, Tabu search, and simulated annealing scales cubically with varying prefactors, with Tabu search exhibiting the lowest prefactor. In contrast, DWave’s runtime scales as \sqrt{n} with n the number of prosumers.

When using the DWave quantum computer to solve a problem, the connectivity of the logical qubits in the problem must be mapped onto the hardware’s connectivity graph, which, for Advantage quantum processing units, is based on the Pegasus graph topology. This mapping process typically necessitates additional qubits, known as physical qubits, beyond those required by the original problem. Figure 3 (c) illustrates the scaling of physical qubits with the number of logical qubits (prosumers).

In Fig. 3 (d), we present the energy distribution (for a randomly generated instance with 100 prosumers) sampled from QAOA enhanced with Fire Opal’s error suppression pipeline [35], DWave, and a random sampler. These distributions correspond to the first split of the grand coalition into two partitions. The vertical cyan line marks the solution found by Gurobi, though its optimality is unproven. Notably, DWave recovers the same solution, while the QAOA distribution closely resembles that of the random sampler. The circuit depth for QAOA in this experiment applying the Fireopal’s transpiler is 11k. Note that no postprocessing is applied to the QAOA output.

IV. CONCLUSION AND OUTLOOK

The formation of energy communities signifies a pivotal shift towards decentralized and sustainable energy man-

agement. In this work, we propose a novel formulation of energy coalition formation that can be encapsulated within the framework of Coalition Structure Generation to comprehend how prosumers can unite in coalitions to maximize their collective advantages. We also introduce a novel method for transforming this formulation into a QUBO formulation for quantum solvers. We then conduct a benchmark comparing classical solvers with quantum solvers in this problem domain. Our findings showcase that the DWave machine outperforms 1-round QAOA on IBM hardware in terms of solution quality. D-Wave exhibits more favorable time scaling with problem size than classical approximate solvers. However, for the system sizes we evaluated, it remains slower than some classical methods, such as QB-Solve. In terms of solution quality, D-Wave matches our best classical solvers (e.g., Gurobi and Tabu Search) for up to 100 prosumers (qubits) and achieves solutions within a 1% optimality gap from Gurobi for problems with 150 prosumers (150 logical qubits).

ACKNOWLEDGMENTS

N.M. and C.O. would like to thank Supreeth Mysore, Ivan Angelov, Stefan Wörner, Antonio Macaluso, Gabriele Agliardi, and Rowen Wu for fruitful discussions. T. M. acknowledges the UK Engineering and Physical Sciences Research Council (EPSRC) (grant reference number EP/Y004418/1).

This work was supported by the German Federal Ministry of Education and Research under the funding program “Förderprogramm Quantentechnologien – von den Grundlagen zum Markt” (funding program quantum technologies — from basic research to market), project Q-Grid, 13N16177.

Supplemental Material

In this Supplemental Material, we provide a brief review of the algorithms that we applied in this work. We also provide further details on the formulation of our energy community formation problem.

I. ALGORITHMS

In this section, we provide a concise overview of the operational mechanisms of classical and quantum algorithms employed in this study.

A. Quantum Algorithms

1. Quantum Annealing

Quantum annealing (QA) is a heuristic algorithm based on the quantum adiabatic theorem [36, 37]. In this algo-

rithm, the system is initially prepared in the ground state of a Hamiltonian H_0 where its ground state is known. A common choice for this initial Hamiltonian is $H_0 = -\sum_{i=1}^N \sigma_i^x$, where N denotes the number of qubits, and the ground state is the uniform superposition of all possible configurations $|+\rangle^{\otimes N}$ with $|+\rangle = (|0\rangle + |1\rangle)/\sqrt{2}$. The Hamiltonian is gradually reweighted to the desired problem Hamiltonian H_C according to

$$H = (1 - \lambda(t))H_0 + \lambda(t)H_C, \quad (S1)$$

where $\lambda(t) \in [0, 1]$ is the annealing schedule. The annealing process can be viewed as H_0 introducing quantum fluctuations originating from the non-commutability of

H_C and H_0 . These fluctuations are gradually reduced to reach the low-energy configuration of the classical energy function H_C . Based on the quantum adiabatic theorem, if one performs the sweep sufficiently slowly, the system remains in its instantaneous ground state throughout the evolution (Fig. S1 (a)) [36, 37]. H_C in our formulation is Eq. (6) at each min cut iteration. The number of qubits is then the number of prosumers. The use of quantum fluctuations in QA has been hypothesized as a potential resource for a speedup over classical methods. Quantum tunneling allows the system to pass through energy barriers that have a higher energy than available in the state [38].

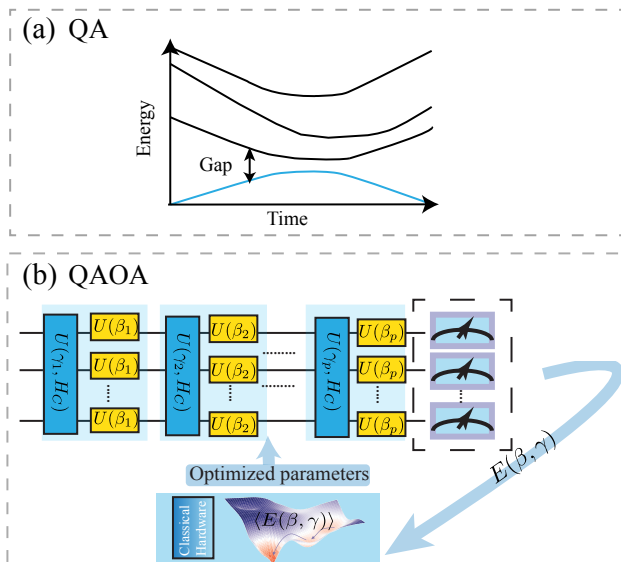


Figure S1. Schematic representation of QA and QAOA.

2. Quantum Approximate Optimization Algorithm

QAOA can be seen as a trotterized version of QA. In QAOA [39], the system is initially prepared in $|+\rangle^{\otimes N}$. Then, unitary operators $U(\gamma_p, H_C) = e^{-i\gamma_p H_C}$ (corresponding to the cost Hamiltonian H_C) and $U(\beta_p) = e^{-i\beta_p H_0}$ (correspond to the mixer Hamiltonian $H_0 = \sum_{i=1}^N \sigma_i^x$) are applied, alternatively, generating the following variational quantum state:

$$|\psi(\boldsymbol{\beta}, \boldsymbol{\gamma})\rangle = e^{-i\beta_p H_0} e^{-i\gamma_p H_C} \dots e^{-i\beta_1 H_0} e^{-i\gamma_1 H_C} |+\rangle^{\otimes N}, \quad (\text{S2})$$

where $\boldsymbol{\gamma} = (\gamma_1, \gamma_2, \dots, \gamma_p) \in [0, 2\pi]^p$ and $\boldsymbol{\beta} = (\beta_1, \beta_2, \dots, \beta_p) \in [0, \pi]^p$ are $2p$ variational parameters and p determines the QAOA depth (number of rounds). Then, a classical optimizer is applied to find the optimal $(\boldsymbol{\beta}, \boldsymbol{\gamma})$ that optimizes the energy expectation $E(\boldsymbol{\beta}, \boldsymbol{\gamma}) = \langle \psi(\boldsymbol{\beta}, \boldsymbol{\gamma}) | H_C | \psi(\boldsymbol{\beta}, \boldsymbol{\gamma}) \rangle$ by updating the variational parameters iteratively (In this study, we applied Cobyala as our classical Optimizer). The parameterized quantum circuit

transfers the initial state to the ground state of the target problem Hamiltonian. Fig. S1 (b) shows the schematic representation of the algorithm.

B. Classical Algorithms

1. Tabu Search

Tabu search is a metaheuristic optimization algorithm [18, 40]. Inspired by the concept of “taboo” this method strategically avoids revisiting previously explored solutions, preventing the algorithm from becoming trapped in local optima. By employing a short-term memory mechanism, Tabu search navigates the solution space by iteratively exploring neighboring solutions while adhering to tabu criteria that guide the search toward promising regions. Its balance between exploration and exploitation makes it a versatile and effective tool for addressing optimization challenges.

2. QB-solve

The QB-solve tackles the challenge of finding the minimum value of large quadratic unconstrained binary optimization (QUBO) problems by breaking them into manageable pieces. It decomposes the global problem into smaller sub-problems by fixing certain bits and optimizing for those with the largest energy impact. This decomposition strategy allows QBsolve to focus on specific regions of the solution space where improvements are likely to have the greatest impact. Each piece is then solved using a specified solver, where here we use the Tabu algorithm [20].

3. Simulated annealing

Simulated annealing [19], inspired by the physical process of annealing in metallurgy, stands as a heuristic tool in the realm of optimization algorithms. At its core, simulated annealing begins with an initial solution and iteratively explores nearby solutions, accepting those that improve upon the current state while occasionally allowing for worse solutions to be accepted probabilistically. This acceptance of inferior solutions is controlled by a temperature parameter, which acts as a guiding force: at higher temperatures, the algorithm is more likely to accept poorer solutions, akin to the exploratory phase of the annealing process. However, as the algorithm progresses, this temperature parameter gradually decreases, reducing the likelihood of accepting suboptimal solutions and guiding the search towards convergence.

4. Gurobi

Gurobi [17] Gurobi is a state-of-the-art commercial solver for a wide range of optimization problems, including linear programming, mixed-integer programming, and quadratic programming. It uses advanced techniques like branch-and-cut, combining the cutting plane method to tighten the solution space and the branch-and-bound algorithm to systematically explore possible solutions. In Gurobi, the optimality gap is defined as the difference between the best solution found by the solver, and the best upper bound estimation of the optimal solution, estimated through the dual problem. A zero gap implies that Gurobi’s solution is exact.

5. Random Sampler

In this work, we apply the random sampler in the dimod package ¹. The random sampler generates a specified number of random configurations (number of shots specified by the user), which represent assignments of values to variables within the problem space defined by the binary quadratic model (BQM). Each configuration serves as a potential solution to the optimization problem. Subsequently, the sampler calculates the objective value for each generated configuration. Among these configurations, the sampler identifies and selects the one with the lowest objective value as the solution.

II. TECHNICAL DETAILS ON PROBLEM FORMULATION

The cost function $c_i(p_i)$ in Eq (1) can be chosen to be either linear or nonlinear, depending on the specific characteristics of prosumers and the energy system. We opt for a linear cost function, $c_i(p_i) = a_i p_i + b_i$, with $a_i = 1$ and $b_i = 0$ for simplicity. This choice may not fully capture all nuances of the prosumer’s behavior and system dynamics. However, it suffices for our purpose.

We establish distinct constraints for agents based on their roles as prosumers, pure consumers, or pure producers at each time. We designate 90 percent of all agents as prosumers, denoting individuals capable of both producing and consuming energy. The remaining 10 percent are randomly assigned as either pure consumers or pure producers. For all prosumers across all time steps, constraints on power levels (p_{it}) in Eq. (1) are established relative to their initial power levels (p_{it}^{initial}). This allows for fluctuations within a defined flexibility ϵ , set to 0.5 here. The initial power of prosumers are sourced from a simulation package that selects a specific location (e.g. Munich) and gathers information, including the number

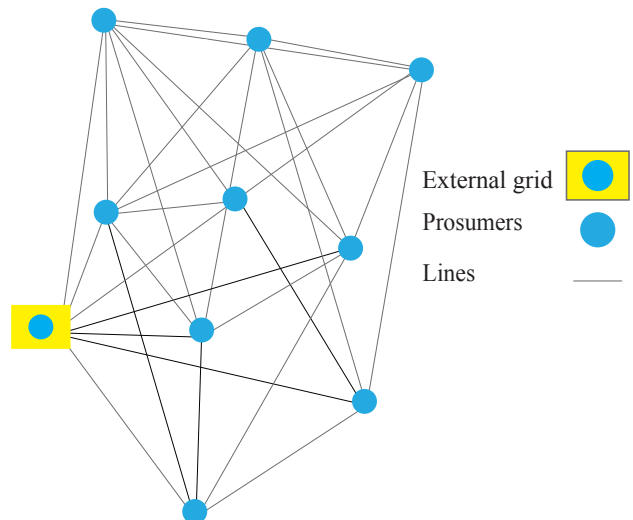


Figure S2. Schematic representation of the network with 9 prosumers and one external grid.

of residential, commercial, and industrial buildings. This data, leveraging standard load profiles and incorporating factors such as the number of households, shops, and industries, as well as their energy usage patterns, enables the estimation of power over time.

For agents that are prosumers, the power is bounded as follows

- When ($p_{it}^{\text{initial}} > 0$):

$$-p_{it}^{\text{initial}}(1 + \epsilon) \leq p_{i,t} \leq p_{it}^{\text{initial}}(1 + \epsilon)$$

- When ($p_{it}^{\text{initial}} < 0$):

$$p_{it}^{\text{initial}}(1 + \epsilon) \leq p_{i,t} \leq -p_{it}^{\text{initial}}(1 + \epsilon)$$

For agents that are pure producers ($p_{it}^{\text{initial}} > 0$) the power is bounded as:

$$0 \leq p_{i,t} \leq p_{it}^{\text{initial}}(1 + \epsilon)$$

For agents that are pure consumers ($p_{it}^{\text{initial}} < 0$) the power is bounded as:

$$p_{it}^{\text{initial}}(1 + \epsilon) \leq p_{i,t} \leq 0$$

The import and export price schedules are established by analyzing the CO_2 intensity derived from real-world data collected in Munich ². In our study, we utilize an external grid, which functions as a Distribution System

¹ <https://docs.ocean.dwavesys.com/en/stable/docsdimod/>

² <https://www.bayernwerk.de/de/fuer-zuhause/oekoheld.html>

Operator (DSO). The external grid acts as a point of connection for exchanging energy to/from prosumers. A schematic representation of our network is shown in Fig. S2. We consider four time steps. Each time step represents a 15-minute interval, capturing a comprehensive one-hour time window.

For power flow optimization, we use Panda Power, a

Python-based library for power systems[41]. We employ the DC optimal power flow (DCPF) method within the Panda Power framework to optimize power flow across the network. Within Panda Power, we model the cost behavior using piece-wise linear (PWL) cost functions. These functions provide a realistic representation of generation costs by capturing nonlinear cost variations.

-
- [1] Amira Abbas, Andris Ambainis, Brandon Augustino, Andreas Bärtschi, Harry Buhrman, Carleton Coffrin, Giorgio Cortiana, Vedran Dunjko, Daniel J Egger, Bruce G Elmegreen, *et al.*, “Quantum optimization: Potential, challenges, and the path forward,” arXiv preprint arXiv:2312.02279 (2023).
- [2] Wayes Tushar, Tapan Kumar Saha, Chau Yuen, M Imran Azim, Thomas Morstyn, H Vincent Poor, Dustin Niyato, and Richard Bean, “A coalition formation game framework for peer-to-peer energy trading,” *Applied Energy* **261**, 114436 (2020).
- [3] Xi Luo and Yanfeng Liu, “A multiple-coalition-based energy trading scheme of hierarchical integrated energy systems,” *Sustainable Cities and Society* **64**, 102518 (2021).
- [4] Jonas Blenninger, David Bucher, Giorgio Cortiana, Kumar Ghosh, Naeimeh Mohseni, Jonas Nüklein, Corey O’Meara, Daniel Porawski, and Benedikt Wimmer, “Quantum optimization for the future energy grid: Summary and quantum utility prospects,” arXiv preprint arXiv:2403.17495 (2024).
- [5] Jonas Nüklein, Daniëlle Schuman, David Bucher, Naeimeh Mohseni, Kumar Ghosh, Corey O’Meara, Giorgio Cortiana, and Claudia Linnhoff-Popien, “Towards less greedy quantum coalition structure generation in induced subgraph games,” arXiv preprint arXiv:2408.04366 (2024).
- [6] David Bucher, Daniel Porawski, Benedikt Wimmer, Jonas Nüklein, Corey O’Meara, Naeimeh Mohseni, Giorgio Cortiana, and Claudia Linnhoff-Popien, “Evaluating quantum optimization for dynamic self-reliant community detection,” arXiv preprint arXiv:2407.06773 (2024).
- [7] Filipe Bandejas, Álvaro Gomes, Mário Gomes, and Paulo Coelho, “Application and challenges of coalitional game theory in power systems for sustainable energy trading communities,” *Energies* **16**, 8115 (2023).
- [8] Milad Moafi, Reza Rouhi Ardeshiri, Manthila Wijesooriya Mudiyansele, Mousa Marzband, Abdullah Abusorrah, Muhyaddin Rawa, and Josep M Guerrero, “Optimal coalition formation and maximum profit allocation for distributed energy resources in smart grids based on cooperative game theory,” *International Journal of Electrical Power & Energy Systems* **144**, 108492 (2023).
- [9] Liyang Han, Thomas Morstyn, and Malcolm McCulloch, “Incentivizing prosumer coalitions with energy management using cooperative game theory,” *IEEE Transactions on Power Systems* **34**, 303–313 (2018).
- [10] Talal Rahwan, Tomasz P Michalak, Michael Wooldridge, and Nicholas R Jennings, “Coalition structure generation: A survey,” *Artificial Intelligence* **229**, 139–174 (2015).
- [11] Yoram Bachrach, Pushmeet Kohli, Vladimir Kolmogorov, and Morteza Zadimoghaddam, “Optimal coalition structure generation in cooperative graph games,” in *Proceedings of the AAAI Conference on Artificial Intelligence*, Vol. 27 (2013) pp. 81–87.
- [12] Xiaotie Deng and Christos H Papadimitriou, “On the complexity of cooperative solution concepts,” *Mathematics of operations research* **19**, 257–266 (1994).
- [13] Talal Rahwan and Nicholas R Jennings, “An improved dynamic programming algorithm for coalition structure generation,” (2008).
- [14] Filippo Bistaffa, Georgios Chalkiadakis, and Alessandro Farinelli, “Efficient coalition structure generation via approximately equivalent induced subgraph games,” *IEEE Transactions on Cybernetics* **52**, 5548–5558 (2022).
- [15] Filippo Bistaffa, Alessandro Farinelli, Jesús Cerquides, Juan Antonio Rodríguez-Aguilar, and Sarvapali D Ramchurn, “Anytime coalition structure generation on synergy graphs,” (2014).
- [16] Supreeth Mysore Venkatesh, Antonio Macaluso, and Matthias Klusch, “Quacs: Variational quantum algorithm for coalition structure generation in induced subgraph games,” arXiv preprint arXiv:2304.07218 (2023).
- [17] Gurobi Optimization, LLC, “Gurobi Optimizer Reference Manual,” (2024).
- [18] Fred Glover, “Future paths for integer programming and links to artificial intelligence,” *Computers & operations research* **13**, 533–549 (1986).
- [19] Scott Kirkpatrick, C Daniel Gelatt Jr, and Mario P Vecchi, “Optimization by simulated annealing,” *science* **220**, 671–680 (1983).
- [20] Michael Booth, Steven P Reinhardt, and Aidan Roy, “Partitioning optimization problems for hybrid classical, quantum execution. Technical Report , 01–09 (2017).
- [21] Humberto Munoz Bauza and Daniel A Lidar, “Scaling advantage in approximate optimization with quantum annealing,” *Phys. Rev. Lett.* **134**.160601 (2025).
- [22] Supreeth Mysore Venkatesh, Antonio Macaluso, and Matthias Klusch, “Bilp-q: quantum coalition structure generation,” in *Proceedings of the 19th ACM International Conference on Computing Frontiers* (2022) pp. 189–192.
- [23] S Thomas McCormick, M Rammohan Rao, and Giovanni Rinaldi, “Easy and difficult objective functions for max cut,” *Mathematical programming* **94**, 459–466 (2003).
- [24] Gavin S Hartnett, Aaron Barbosa, Pranav S Mundada, Michael Hush, Michael J Biercuk, and Yuval Baum, “Learning to rank quantum circuits for hardware-optimized performance enhancement,” arXiv preprint arXiv:2404.06535 (2024).
- [25] Nic Ezzell, Bibek Pokharel, Lina Tewala, Gregory Quiroz, and Daniel A. Lidar, “Dynamical decoupling for superconducting qubits: A performance survey,” *Phys. Rev. Appl.* **20**, 064027 (2023).
- [26] Atsushi Matsuo, Shigeru Yamashita, and Daniel J Egger, “A sat approach to the initial mapping problem in swap gate insertion for commuting gates,” *IEICE Transactions*

- on Fundamentals of Electronics, Communications and Computer Sciences **106**, 1424–1431 (2023).
- [27] Johannes Weidenfeller, Lucia C Valor, Julien Gacon, Caroline Tornow, Luciano Bello, Stefan Woerner, and Daniel J Egger, “Scaling of the quantum approximate optimization algorithm on superconducting qubit based hardware,” *Quantum* **6**, 870 (2022).
- [28] David Amaro, Carlo Modica, Matthias Rosenkranz, Matia Fiorentini, Marcello Benedetti, and Michael Lubasch, “Filtering variational quantum algorithms for combinatorial optimization,” *Quantum Science and Technology* **7**, 015021 (2022).
- [29] Yunlong Yu, Chenfeng Cao, Carter Dewey, Xiang-Bin Wang, Nic Shannon, and Robert Joynt, “Quantum approximate optimization algorithm with adaptive bias fields,” *Phys. Rev. Res.* **4**, 023249 (2022).
- [30] Leo Zhou, Sheng-Tao Wang, Soonwon Choi, Hannes Pichler, and Mikhail D. Lukin, “Quantum approximate optimization algorithm: Performance, mechanism, and implementation on near-term devices,” *Phys. Rev. X* **10**, 021067 (2020).
- [31] Vishwanathan Akshay, Daniil Rabinovich, Ernesto Campos, and Jacob Biamonte, “Parameter concentrations in quantum approximate optimization,” *Physical Review A* **104**, L010401 (2021).
- [32] JA Montanez-Barrera, Dennis Willsch, and Kristel Michielsen, “Transfer learning of optimal qaoa parameters in combinatorial optimization,” arXiv preprint arXiv:2402.05549 (2024).
- [33] Naeimeh Mohseni, Junheng Shi, Tim Byrnes, and Michael Hartmann, “Deep learning of many-body observables and quantum information scrambling,” arXiv preprint arXiv:2302.04621 (2023).
- [34] Naeimeh Mohseni, Carlos Navarrete-Benlloch, Tim Byrnes, and Florian Marquardt, “Deep recurrent networks predicting the gap evolution in adiabatic quantum computing,” *Quantum* **7**, 1039 (2023).
- [35] Natasha Sachdeva, Gavin S Harnett, Smarak Maity, Samuel Marsh, Yulun Wang, Adam Winick, Ryan Dougherty, Daniel Canuto, You Quan Chong, Michael Hush, *et al.*, “Quantum optimization using a 127-qubit gate-model ibm quantum computer can outperform quantum annealers for nontrivial binary optimization problems,” arXiv preprint arXiv:2406.01743 (2024).
- [36] Edward Farhi, Jeffrey Goldstone, Sam Gutmann, and Michael Sipser, “Quantum computation by adiabatic evolution,” arXiv preprint quant-ph/0001106 (2000).
- [37] Tameem Albash and Daniel A. Lidar, “Adiabatic quantum computation,” *Rev. Mod. Phys.* **90**, 015002 (2018).
- [38] Vasil S Denchev, Sergio Boixo, Sergei V Isakov, Nan Ding, Ryan Babbush, Vadim Smelyanskiy, John Martinis, and Hartmut Neven, “What is the computational value of finite-range tunneling?” *Physical Review X* **6**, 031015 (2016).
- [39] Edward Farhi, Jeffrey Goldstone, and Sam Gutmann, “A quantum approximate optimization algorithm,” arXiv preprint arXiv:1411.4028 (2014).
- [40] Gintaras Palubeckis, “Multistart tabu search strategies for the unconstrained binary quadratic optimization problem,” *Annals of Operations Research* **131**, 259–282 (2004).
- [41] Leon Thurner, Alexander Scheidler, Florian Schäfer, Jan-Hendrik Menke, Julian Dollichon, Friederike Meier, Steffen Meinecke, and Martin Braun, “pandapower—an open-source python tool for convenient modeling, analysis, and optimization of electric power systems,” *IEEE Transactions on Power Systems* **33**, 6510–6521 (2018).